

Ground Vortex Formed by Impinging Jets in Crossflow

K. Knowles* and D. Bray†

Royal Military College of Science (Cranfield Institute of Technology),
Shrivenham, Swindon,
Wiltshire SN6 8LA, England, United Kingdom

The flowfields associated with single and twin jets impinging in crossflows have been studied experimentally using ground plane pressure profiles and flow visualization. The following parameters and their effect on the position of the ground vortex have been investigated: crossflow-to-jet velocity ratio, crossflow boundary-layer thickness, nozzle height, nozzle pressure ratio, vector angle, and nozzle splay with both fixed and moving ground planes. Results show that the ground vortex moves away from the nozzle centerline as crossflow-to-jet velocity ratio is decreased; the rate of change of position, however, depends on other parameters. This article presents an analysis of this experimental data which isolates the effects of these individual parameters. Nozzle pressure ratio is seen to influence ground vortex position independently of velocity ratio, but the definitions of jet equivalent velocity and crossflow velocity ratio are shown to be important. The effect of the moving ground plane is to reduce vortex penetration significantly; this suggests that a moving ground plane simulation (or moving model) is essential when testing design configurations in ground effect in wind tunnels. With twin nozzles there is a distinct effect of nozzle height on the upstream extent of the ground sheet, especially when the nozzles are toed-in. It is suggested that the twin nozzle height effect is connected with jet merging. It is also argued that rig design can produce a blockage effect which moves the ground vortex significantly and can change other apparent parametric effects.

Nomenclature

A_n = nozzle exit area
 C_p = pressure coefficient, $(p - p_\infty)/(\frac{1}{2}\rho_\infty V_\infty^2)$
 d_n = nozzle exit diameter
 h = height of nozzle above ground, (Fig. 2)
 p = pressure
 pr_n = nozzle pressure ratio, p_0/p_∞
 T = thrust
 V = velocity
 V_E = as V_e but using thrust-based w_{c1}
 V_e = effective velocity ratio, $\sqrt{\frac{1}{2}\rho_\infty V_\infty^2}/(\frac{1}{2}\rho_1 w_{c1}^2)$
 v = y direction velocity
 w = jet velocity
 x = horizontal distance measured normal to the crossflow from the plane of symmetry
 y = horizontal distance measured upstream from the nozzle centerline, (Fig. 2)
 y_p = position of peak C_p upstream of ground vortex
 y_s = position at which mean $C_p = 0$
 y_v = position of minimum C_p (under vortex core)
 z = vertical distance above the ground plane
 δ = crossflow boundary-layer thickness
 ρ = density

Subscripts

c = maximum
 g = ground plane
 i = impingement
 w = wall jet
 ∞ = ambient (crossflow) conditions

0 = jet stagnation conditions
1 = nozzle exit conditions

Introduction

WHEN a jet impinges on a surface normal (or nearly normal) to its axis, a wall jet is formed which spreads out radially from the impingement point. In the presence of a crossflow (parallel to the wall) the wall jet will eventually separate and roll up to form a vortex arranged as a horseshoe around the impingement point (Figs. 1 and 2). This so-called ground vortex flowfield is of particular interest in the development of advanced short take off and vertical landing (AS-TOVL) aircraft, where it can influence both airframe air loads and engine intake flows. Therefore, there is a need to model this flowfield, both experimentally and numerically. Both have been done before,¹⁻¹⁴ at least over a more or less limited range of conditions, but there are problems with this data base. There is considerable scatter in the experimental data (Fig. 3); the end result of the scale model tests in the aircraft industry—the level of engine hot gas ingestion—is known to scale very poorly to full size; as a consequence of both of these there are little or no reliable experimental data against which to validate the computational fluid dynamic (CFD) models, especially at high jet pressure ratios. The present work is aimed at a better understanding of single- and twin-jet impingement in crossflows and, in particular, at isolating parametric effects on ground vortex formation.

The upwind extent of the ground vortex can be determined experimentally either by flow visualization^{1-4,10} or from surface pressure plots.⁶⁻⁹ Such a plot in the plane of symmetry of the ground vortex is sketched in Fig. 4. This reveals three key points representative of the vortex position: 1) y_v , 2) y_s , and 3) y_p . These are generally taken to correspond^{2,6} to the positions of the vortex core, the separation point, and the maximum penetration point, respectively. It has been shown^{11,15} that there is a fixed linear relationship between y_v , y_s , and y_p , and so any one of these can be taken to be indicative of the vortex position. For the present work, y_s has generally been chosen, since it is easier to determine this position accurately.

Presented as Paper 91-0768 at the AIAA 29th Aerospace Sciences Meeting, Reno, NV, Jan. 7-10, 1991; received Sept. 3, 1991; revision received Aug. 21, 1992; accepted for publication Aug. 29, 1992. Copyright © 1992 by K. Knowles and D. Bray. Published by the American Institute of Aeronautics and Astronautics, Inc., with permission.

*Senior Lecturer, Aeromechanical Systems Group. Member AIAA.

†Lecturer, Aeromechanical Systems Group. Member AIAA.

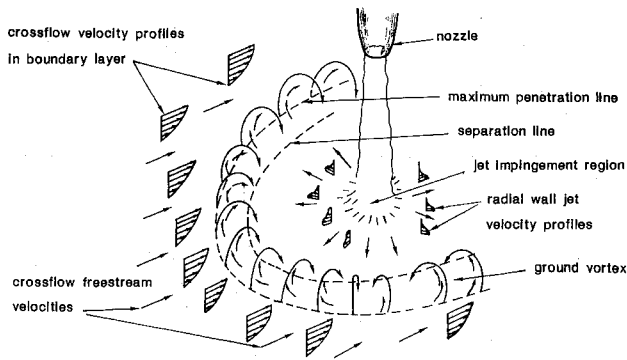


Fig. 1 Ground vortex formed by impinging jet in crossflow.

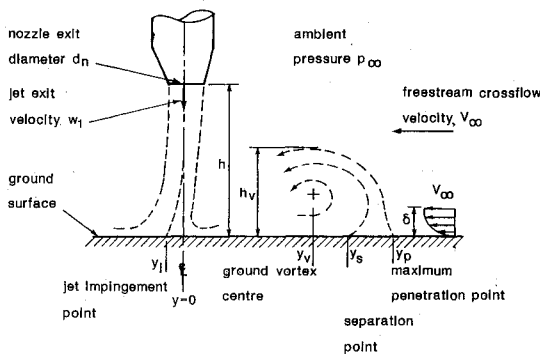


Fig. 2 Plane of symmetry for single impinging jet in crossflow.

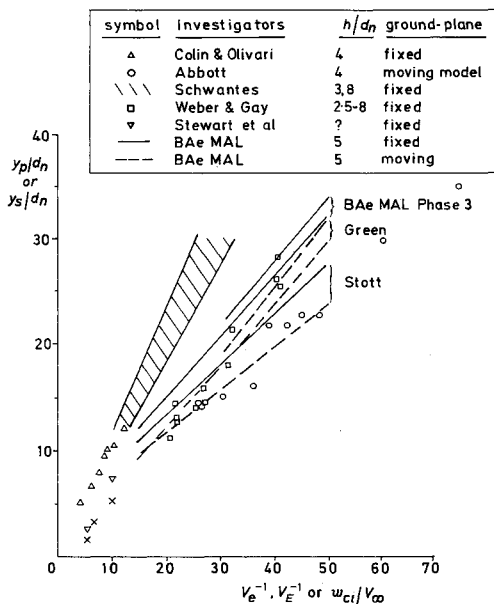


Fig. 3 Normalized vortex penetration against effective velocity ratio—comparison of previous investigations.

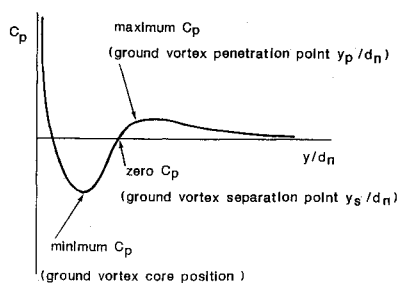


Fig. 4 Typical ground vortex static pressure distribution.

Comparisons with other workers, however, can be difficult, especially where they have used flow visualization.

The present work has set out to determine experimentally the effect on the ground vortex position of a number of parameters: nozzle height ($h/d_n = 2$ to 10), nozzle pressure ratio ($pr_n = 1.05$ to 4), crossflow-to-jet velocity ratio ($V_e = 0.1$ to 0.013), and vector angle (-5 to $+10$ deg) for single- and twin-jet configurations with both fixed and moving ground planes (simulating ambient wind or aircraft motion). For the (side-by-side) twin-jet configurations, the effect of nozzle splay has also been investigated. Some of these parametric trends have been published previously,¹⁵ the more important of these will be emphasized here before the latest results are discussed.

Experimentation

A schematic of the experimental layout is shown in Fig. 5. The Royal Military College of Science (RMCS) open-jet wind tunnel (OJWT), having a 1.1×1.5 m elliptical nozzle, supplies the crossflow with a maximum wind speed of 42 ms^{-1} . In the working section is a removable "rolling road" (1.1×1.7 m) with a boundary-layer suction slot upstream. To prevent the rolling-road belt from flapping or lifting off its base, belt suction is provided. This is arranged in four separate full-span sections; the level of suction in each section can be varied independently. It is therefore possible to increase the belt suction under the forward part of the vortex (where considerable "lift" was experienced) while suction is reduced under the impingement point. Even so, the combination of lift under the front of the vortex and a large download under the jet impingement can provide a limit to the test conditions available with the rolling road on, especially if large nozzles are used.

Ambient-temperature compressed air for the jet is provided by two screw-type compressors by way of a 34-m^3 storage tank. This system allows a 1-in.- (25.4-mm-) diam nozzle to be run continuously at up to $pr_n = 7$, or two such nozzles at up to $pr_n = 4$. Larger nozzles could, of course, be run intermittently. The compressed air is connected to a settling chamber (approximately 340-mm wide, 140-mm deep, and 150-mm high, externally) in the OJWT test section. One or two nozzles can be fitted to the lower surface of this plenum. By incorporating different designs of lower plate, nozzle vector (fore and aft angle) and splay or toe-in (differential transverse angle) can be incorporated. When comparing vectored and unvectored test results, it should be noted that the perpendicular height (in nozzle diameters) from the ground plane to the center of the nozzle exit planes was the same in each case. Similarly, with different splay (or toe-in) angles, the distance between the two nozzle centerlines at exit was maintained at three diameters. For all the results presented here, simple conical nozzles of $d_n = 0.5$ in. (12.7 mm) were used having a convergence of length $d_n/4$ and a total length of $10d_n$. These are referred to here as the "long $\frac{1}{2}$ -in. nozzles." Reference 15 discusses other nozzles tested.

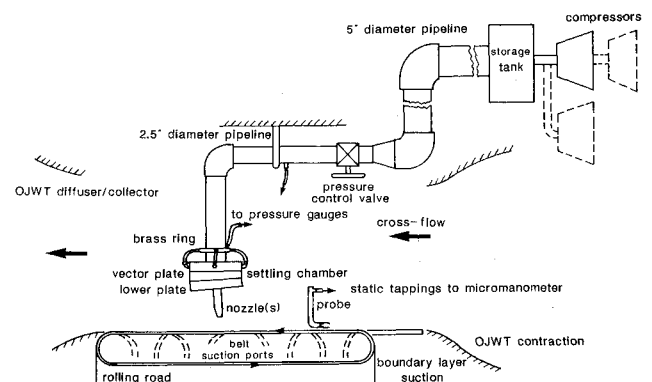


Fig. 5 General arrangement of the experimental setup.

Ground plane static pressures were measured using a pitot-static tube aligned with the crossflow and traversed in the streamwise direction. The traverse plane was the plane of symmetry of the flowfield. The probe was positioned as close as possible to the ground surface (typically 4 mm to the centerline of a 4-mm-diam probe), without being noticeably affected by any ground belt flapping. This "standoff probe" technique has been validated by comparison with fixed ground board static tapings; the only measureable errors involved are under the ground vortex⁸ where, as expected, the probe gives a lower static pressure. The measured positions of y_p , y_s , and y_v , however, are not significantly affected by the use of the probe.

Smoke flow visualization has also been used in the present work. For this, a separate, small-scale rig has been built¹⁶ with smoke injected into the compressed air supply. Only low jet pressure ratios can be investigated with this facility. Comparisons between the flow visualization and pressure traverses show reasonably good agreement (based on y_p). For the single nozzle the largest difference in penetration is $2d_n$, with a uniform scatter of data, except at $h/d_n = 8$ where the flow visualization consistently gives more penetration. For the twin nozzle tests there is more data scatter (up to $5d_n$), and $h/d_n = 8$ data all show a reduced penetration.

Results and Discussion

As discussed earlier,^{11,15} self-similarity laws appear to exist for the ground vortex, at least in the plane of symmetry (Fig. 6). This allows any one of the positions y_p , y_s , or y_v to be used to quantify vortex position. Static pressure traverses conducted in the twin nozzle plane of symmetry revealed a similar distribution to that found in the single nozzle cases, but with no minimum C_p detected within the traverse range. The absence of an apparent vortex does not prevent separation and penetration distances (y_s and y_p) being quantified. When plotted on the same basis as Fig. 6, the same self-similarity is revealed as for the single nozzle. It should be recognized that the plane of symmetry of the twin-jet flowfield, especially close to the nozzles, already contains a separated shear layer (the fountain) and that within this sheet static pressures are subatmospheric.¹⁷

The current experimental work has been conducted in two phases, including some deliberate overlap to assess experimental repeatability. Comparison between these repeated test points is presented in Fig. 7. This shows a scatter of up to $1d_n$. By comparison, Stott⁹ found a similar level of repeatability for a similar range of penetration distances. From this it is concluded that variations of vortex position of less than 5% are unlikely to be parametric effects, and that apparent trends of up to 13% could be random if based on only one

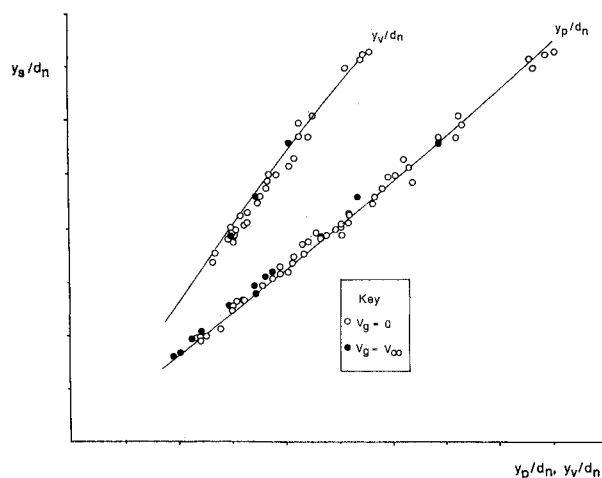


Fig. 6 Ground-vortex self-similarity.

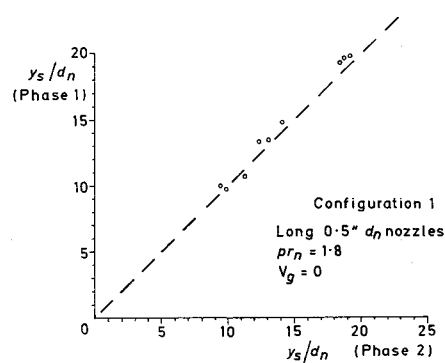


Fig. 7 Experimental repeatability.

data point (deduced from statistical analysis of Stott's⁹ multiple tests). Comparisons between different workers' results for similar conditions,¹⁵ however, can show a far greater scatter than this, even when the same rig is used.^{8,9} This perhaps illustrates the sensitivity of this flowfield to minor changes in various parameters.

Effect of Crossflow Velocity Ratio

An important parameter in analyzing test results has been found to be the crossflow velocity ratio. This is defined here as

$$V_e = \sqrt{\frac{1}{2} \rho_\infty V_\infty^2 / (\frac{1}{2} \rho_1 w_{c1}^2)} \quad (1)$$

where w_{c1} is defined as the velocity which would exist at the exit of a fully-expanded convergent-divergent nozzle operated at the same pressure ratio as the convergent nozzle. Some authors, however, use a thrust-based equivalent nozzle velocity, thus

$$w_{c1} = \sqrt{(T/2\rho_1 A_n)} \quad (2)$$

The crossflow velocity ratio is also defined by many authors simply as w_{c1}/V_∞ , and it has previously been shown⁷ that this latter definition appears to lead to poorer data collapse when plotting against the crossflow velocity ratio and including data for underexpanded nozzle pressure ratios.

Whichever definition of V_e is used, vortex penetration is found to increase as V_e^{-1} increases (Fig. 3). The rate of increase, however, depends on other parameters and on the precise definition of V_e . Much of the scatter between different authors in Fig. 3 is felt to be due to different V_e definitions. Even when the same definition is used, as with the data of Green⁸ and Stott,⁹ there is a marked scatter. As discussed above, this is not just a problem with experimental repeatability, but presumably illustrates the impact of other parameters. Even though there is poor repeatability between Green's and Stott's data for individual points, this is not necessarily reflected by the *average* lines of Fig. 3, since, for instance, these are averaged over different pressure ratio ranges. Therefore, it is strongly recommended that, although V_e is an important parameter in determining the ground vortex flowfield, it is not the only one, and general plots against V_e are meaningless. In particular, no meaningful single correlation of y_s (or y_p) against V_e^{-1} can be produced.

The same general trend with V_e is seen with twin nozzles, as was the case for the single nozzle. As shown in Fig. 8, however, penetration is increased with twin nozzles, even over that expected of a single nozzle of the same total exit area. However, as flow visualization¹⁶ reveals (Fig. 9), this increased penetration is confined to the central upwind portion of the vortex where the twin-jet fountain projects forward of the main vortex. Away from this region the twin- and single-nozzle flowfields are virtually identical, suggesting a shielding effect of one jet on the other. It should be pointed out that

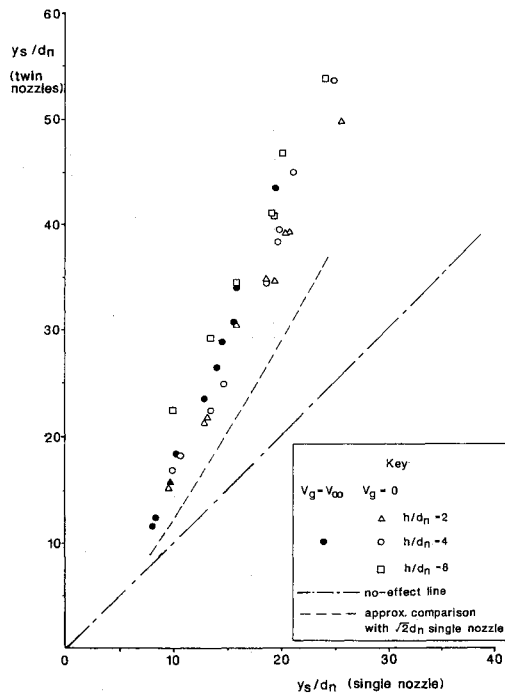


Fig. 8 Comparison of twin nozzle and single nozzle separation distances (long 0.5-in. nozzles).

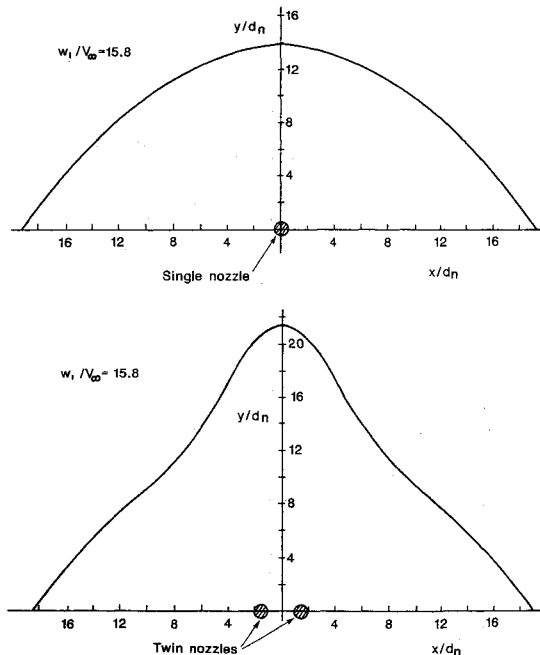


Fig. 9 Locus of ground sheet forward penetration for single and twin nozzles (flow visualization studies).

the twin nozzle vortex locus shown in Fig. 9 may be strongly dependent on the nozzle spacing used here ($3d_n$). Wider spacings do not appear to produce a spike on the locus in this central upwind region.^{18,19}

Effect of Moving Ground Plane and Crossflow Boundary Layer Thickness

The present tests confirm⁷ that the use of a rolling road consistently produces a reduction in vortex penetration compared with the fixed ground plane, as shown in Fig. 10. This reduction in penetration is presumably due to the reduction in crossflow momentum deficit produced by using the rolling road (Fig. 11), and/or the increased wall jet shear stress. Which of these, if either, is the dominant effect is not clear:

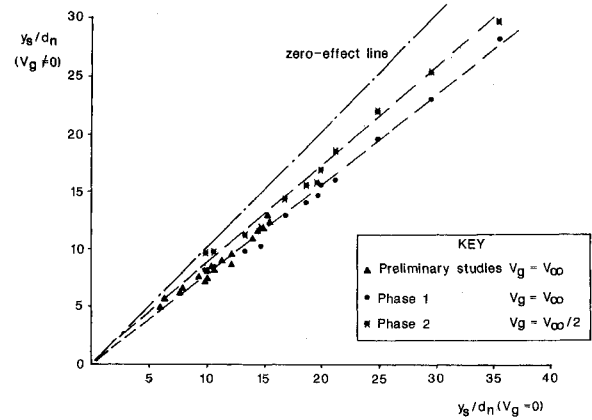


Fig. 10 Effect of rolling road on separation distance.

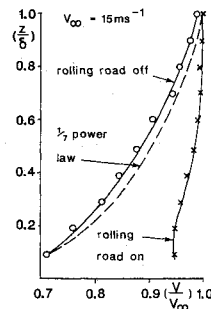


Fig. 11 Effect of rolling road on crossflow boundary layer.

experiments elsewhere suggest that small changes in crossflow boundary-layer thickness (of the order of a few nozzle diameters) have only a small effect on vortex position⁶; large boundary-layer thicknesses, however, do cause an increase in vortex penetration.¹⁵ It seems most likely, however, that the increased wall jet shear stress plays a significant part in this effect, and that tunnel floor boundary-layer control will be insufficient to model aircraft motion through still air.

The effect of a small change in crossflow boundary-layer thickness is shown in Fig. 12. With a 1-in.- (25.4-mm-) diam nozzle (total length $5d_n$) the crossflow boundary layer is about $1d_n$ thick; with a $1/2$ -in. (12.7-mm) nozzle (total length $10d_n$) this is doubled. It can be seen that there is no consistent effect of this increased boundary-layer thickness, although there is a general trend towards increased penetration which is somewhat greater than the general experimental scatter. It should be noted that with the smaller d_n nozzle, the plenum is 2-in. (50.8-mm) closer to the ground under these conditions: this will have a slight effect on penetration, but less¹⁵ than that shown in Fig. 12.

Twin parallel nozzles show the same rolling road effect as the single nozzle; this is not so if the nozzle centerlines are converging (nozzle toe-in). In these cases the average y_p reduction was found to be about 30% less than with the normal jets. This seems to be a function of jet merging, but it is an average statement and, again, it hides some complex effects. For instance, for these toed-in configurations there is some indication that at lower penetrations there is a greater rolling-road effect than the average; or there could just be increased data scatter in these twin nozzle tests.

As indicated in Fig. 10, tests have also been conducted with the rolling road running at half the freestream speed. These show a reduction in vortex penetration, but not half that seen when $V_g = V_\infty$. In principle, this allows the relative contributions of wall jet shear stress and crossflow momentum deficit to be assessed if certain simplifying assumptions are made. From the point of view of wind-tunnel model tests on AS-TOVL configurations, however, the mechanism by which the vortex penetration changes is not of immediate importance;

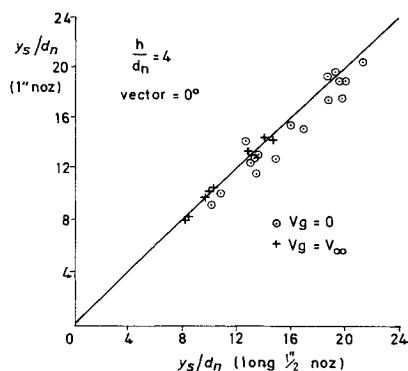


Fig. 12 Effect of crossflow boundary-layer thickness on vortex penetration.

what is important is that a rolling vertical landing must be simulated using a rolling-road or moving model.

Effect of Nozzle Height

Nozzle height seems to be an extremely difficult parametric effect to isolate reliably. For a single nozzle, the traditional description of vortex sensitivity to nozzle height has an initial increase in penetration as nozzle height is increased, apparently due to more efficient turning in the impingement region with high nozzles (and therefore, lower impingement velocities) giving lower loss of momentum on entering the wall jet. This is followed by a reduction in y_p as the jet deflects in the crossflow, deflection being limited at low heights by vortex blockage. This sort of behavior was shown by Schwantes⁴ for low pr_n jets, and by Stott⁹ for a range of pr_n up to underexpanded. Cimbalá et al.⁶ show an increase in y_p (relative to the impingement point) for height increases from 1 to $4d_n$ at $V_\infty/w_{c1} = 0.1$, but only a decrease in penetration at $V_\infty/w_{c1} = 0.3$ ($h < 3d_n$ in this case). For multiple jets, MacLean et al.¹⁰ show no height effects at higher velocity ratios ($V_\infty/w_{c1} > 0.1$) with a height dependence at lower velocity ratios (< 0.06).

The current authors have previously shown results¹⁵ which tend to support the view that (for $h/d_n < 8$) there is little consistent effect of nozzle height for single nozzles across a range of pr_n . This has been modified somewhat by extra experimental results (only at $pr_n = 1.8$), including some at $h = 10d_n$, as shown in Fig. 13. Also shown in this figure are results from Stott,⁹ but a direct comparison with the present work is not very meaningful because of the different definitions of velocity ratio used between the two sets of data and the fact that Stott's curves are averaged over various pressure ratios. As discussed previously,¹⁵ Stott's height effect is also susceptible to a variable and unknown rig interference (likely to be of the order of $3d_n$ ¹⁵). The important feature of the rig used by Stott was the nose fairing, which extended approximately $11d_n$ forward of the nozzle centerline. This almost certainly influenced the vortex flowfield (even for y_s of the order of $20d_n$) and, in this case, may have caused an underpenetration of the vortex at low rig heights. This trend was illustrated by Cimbalá et al.⁶ who introduced a plate in the plane of the nozzle exit, parallel to the ground, and showed a reduction in vortex penetration. It is important from the point of view of wind-tunnel testing to note that the influence of nozzle height on vortex position can be rig-dependent.

The current twin nozzle tests have shown a marked effect of nozzle height on penetration.¹⁵ Over the height range of $2-8d_n$, the twin parallel nozzles showed penetration increases varying between 1–10 diameters, but with the majority of cases showing an increase of penetration between $4-8d_n$. This is generally a bigger change in penetration than caused by rig blockage. It is not clear exactly what is the mechanism causing this effect; it may be associated with the fountain flow, in which case nozzle spacing may also have an influence. It has been suggested by the authors¹⁵ that jet merging may have

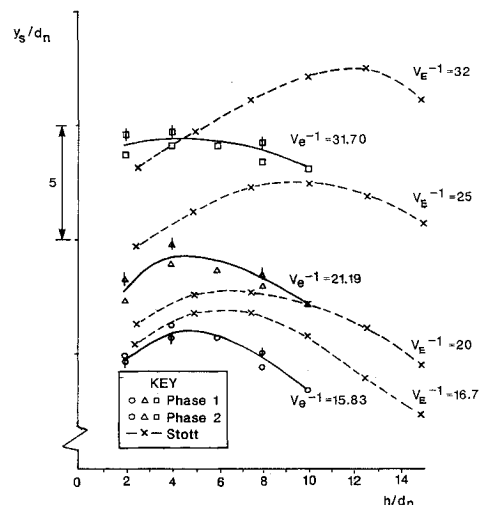


Fig. 13 Effect of height on separation distance (single nozzle).

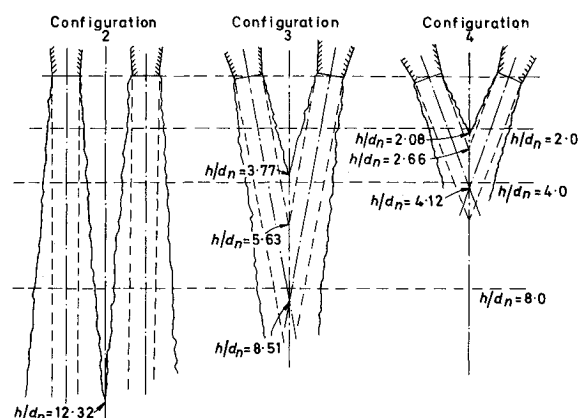


Fig. 14 Merging of twin jets.

an influence. For the current spacing of $3d_n$ and assuming a jet spreading angle of 7 deg (the spreading rate of the $w_c/2$ line deduced from Ref. 20), simple geometry suggests that the two jets will start to merge at about $12d_n$ (this is illustrated in Fig. 14). This spreading rate, however, is deduced from data for an isolated jet, it is conceivable that two closely spaced jets will spread faster due to mutual interference, or will bend in towards each other. Only a slight increase in spreading angle is needed for the edges of the two jets to merge at $h = 8d_n$, which is the height of peak penetration for two parallel jets.

When the twin nozzles are toed-in (Fig. 14), there is a dramatic height effect (Figs. 15 and 16). For moderate toe-in (Fig. 15), penetration increases up to $h = 4d_n$, after which the "spike" on the ground vortex collapses and the vortex locus looks like that from a single jet (indeed, the penetration is virtually identical to that from a single nozzle of the same total exit area at the same conditions). The peak penetration occurs at roughly the same height as that for jet merging (Fig. 14). At the higher toe-in angle (Fig. 16) the same is true: maximum penetration just as the edges of the jets are merging, followed by a single jet-like locus once the jet centerlines merge. Note that in this latter case there is a dramatic reduction in penetration as height is increased above that for jet centerline confluence, resulting (at $h/d_n = 8$) in less penetration than for a single nozzle under the same conditions. This reduction is presumably due to an increase in momentum loss caused by jet impact.

Effect of Nozzle Pressure Ratio

Few of the previous workers have looked at pr_n effects. The results of Stott⁹ show a general, although not consistent,

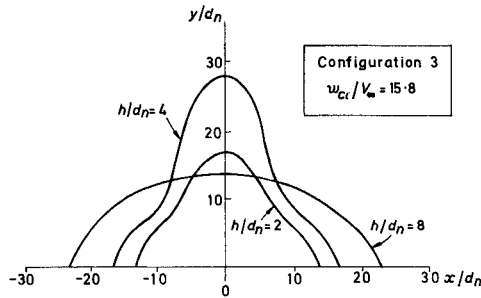


Fig. 15 Locus of ground sheet forward penetration for twin nozzles with moderate toe-in.

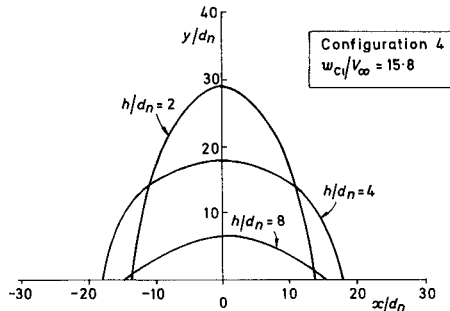


Fig. 16 Locus of ground sheet forward penetration for twin nozzles with substantial toe-in.

trend with penetration increasing as pressure ratio increases from 1.5 to 3, followed by a decrease, or little change, in penetration up to $pr_n = 4$. The present results (Fig. 17) show a consistent trend (albeit over a more limited range of conditions than Stott's): penetration increases up to choking (probably peaking just beyond $pr_n = 2$), decreases up to $pr_n = 2.5$, and then peaks again close to $pr_n = 3$. Very similar pressure ratio effects are seen with twin nozzles (the only significant difference occurs at the highest height tested where there is relatively little increase in penetration up to choking). This is, at least, consistent with the changes in shock pattern which occur over this pressure ratio range,²⁰ but is markedly different from the trends shown by Stott.⁹ Part of the explanation seems to lie in the definitions of w_{c1} and V_e . Stott used measured thrust to calculate an equivalent w_{c1} which may have been ratioed directly with V_{∞} to produce his V_E^{-1} . We use a fully expanded velocity and ratio the square roots of dynamic pressures. However, Stott has defined his V_E , we find that at pressure ratios of 3 and 4 he has a lower value of V_E^{-1} than our V_e^{-1} , for the same conditions. His curves, therefore, jump from a low V_e^{-1} (e.g., 40) in Fig. 17 to a higher value (e.g., 50) at $pr_n = 3$. At low vortex penetrations there is also the likelihood of rig interference effects in the results of Ref. 9.

Effect of Nozzle Vector Angle

The effect of vectoring the nozzle is shown in Fig. 18. Three vector angles have been considered, -5° , $+5^\circ$, and $+10^\circ$, the sign convention being indicated on the figure. In each case, the origin for y is the intersection of the nozzle centerline with the ground plane. A forward vector of -5° causes an increase in penetration of about 15%, with a rearward vector of $+5^\circ$ giving a similar decrease, compared with the normal impinging jet. Ten-deg rearward vector gives a 23% reduction in penetration. (The trend lines indicated in Fig. 18 are for the single-nozzle results only.) Note that the vortex self-similarity is not affected by vectoring. It is assumed that the effect of the rolling road is uniformly additive to that of nozzle vector.

The twin parallel nozzle vector results are also shown in Fig. 18. For 5° -deg vector, the twin-nozzle configuration shows very similar trends to those for the single nozzle. The results for $+10^\circ$ deg, however, show more underpenetration and far

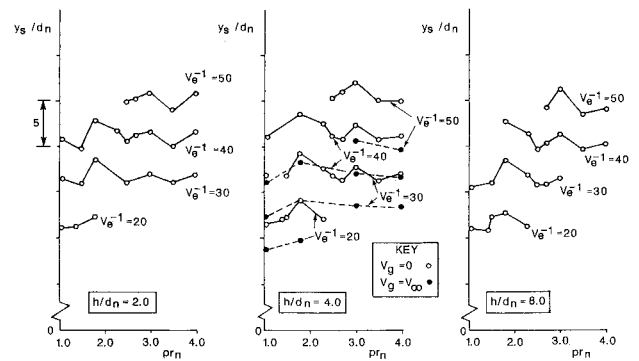


Fig. 17 Effect of pressure ratio on separation distance (long 0.5-in. single nozzle).

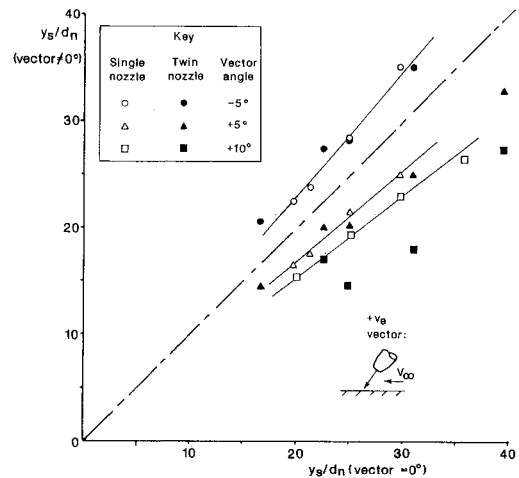


Fig. 18 Effect of vector angle on separation distance (long 0.5-in. nozzles).

less linear behavior than the single nozzle. There appears to be a "kink" in all the twin-nozzle trends at a nonvectored separation distance of $22-25d_n$; either side of this the twin nozzle data tend to run parallel with those for the single nozzle. What might be causing this is not clear: the kink could be a problem with the unvectored data; or there could be insufficient data points to be sure that it is a significant trend.

Conclusions

An experimental investigation has been made into the parameters which affect the position of the ground vortex formed by single- and twin-impinging jets in crossflow. It has been confirmed that there is a constant relationship between the penetration distance, the separation distance, and the position of the vortex core, thus, any one of these can be used to quantify ground sheet forward penetration. The relationship between y_p and y_s seems to hold for single and twin nozzles across the complete range of parameters tested. In terms of y_s , the following trends have been found:

1) Penetration increases with increasing V_e^{-1} , but the rate depends on other parameters. Consequently, it is felt that a universal law does not exist to link penetration and velocity ratio.

2) Penetration decreases when a moving ground plane is used, due to reduced crossflow momentum deficit and increased wall jet shear stress. Since this latter seems to play a significant role in this effect, it precludes the use of tunnel-floor boundary-layer control in simulating STOVL aircraft motion in ground proximity.

3) The effect of nozzle height for single jets is seen to be difficult to isolate, and some previous results showing an effect are thought to be rig-dependent. There is some evidence here to show an initial increase in penetration with increasing height,

followed by a reduction at high nozzle heights as jet deflection increases.

4) There is an increase of penetration with height for twin jets, and this seems to be associated with the edges of the jets merging. For toed-in nozzles this is also true, but after the jet centerlines have merged there is a dramatic reduction in penetration.

5) Penetration increases with nozzle pressure ratio (at constant V_e) up to just beyond choking, it decreases at higher pressure ratios, but with a second, lower peak around $pr_n = 3$.

6) This pressure ratio trend is consistent with shock structure changes, but relies on using a fully expanded equivalent jet velocity and a velocity ratio based on dynamic pressures. Other velocity ratios give poorer data collapse, and thrust-based equivalent velocities give a pressure ratio trend which is not consistent with shock structures.

7) Vectoring the nozzles forwards increases penetration (relative to the geometric impingement point) and rearward vectoring gives a reduction: 15% for 5 deg and 23% for 10 deg.

8) Overall twin side-by-side parallel nozzles (of $3d_n$ spacing) give a greater penetration than equivalent single nozzles, although flow visualization suggests that this is confined to the central, upwind portion of the ground sheet.

The current experimental studies have found the flowfield to be extremely unsteady, especially in the presence of the twin-jet fountain flow. This unsteadiness is now being investigated experimentally as it is recognized as being crucial to the engine's response to hot gas ingestion.

Acknowledgments

The authors wish to thank British Aerospace (Military Aircraft) Ltd., and in particular, P. Curtis and P. G. Knott for their help with the current work. Much of this work has been funded by BAe but the views expressed are the authors' own.

References

- ¹Abbott, W. A., "Studies of Flowfields Created by Vertical and Inclined Jets when Stationary or Moving over a Horizontal Surface," Aeronautical Research Council, CP 911, UK, Oct. 1964.
- ²Colin, P. E., and Olivari, D., "The Impingement of a Circular Jet Normal to a Flat Surface With and Without Crossflow," U.S. Army European Research Office, AD 688-953, von Karman Institute, Brussels, Belgium, Jan. 1969.
- ³Webber, H. A., and Gay, A., "VTOL Reingestion Model Testing of Fountain Control and Wind Effects," AIAA/SAE 11th Propulsion Conf., AIAA Paper 75-1217, Anaheim, CA, Sept./Oct. 1975.
- ⁴Schwantes, E., "The Recirculation Flow Pattern of a VTOL Lift-Engine," NASA TT F-14912, June 1973.
- ⁵Stewart, V. R., Kuhn, R. E., and Walters, M. M., "Characteristics of the Ground Vortex Developed by Various V/STOL Jets at Forward Speed," AIAA Aircraft Design, Systems and Technology Meeting, AIAA Paper 83-2494, Ft. Worth, TX, Oct. 1983.
- ⁶Cimbala, J. M., Stinebring, D. R., Treaster, A. L., and Billet, M. L., "Experimental Investigation of a Jet Impinging on a Ground Plane in the Presence of a Cross-Flow," *Proceedings of the International Powered Lift Conference*, Paper 872326, Santa Clara, CA, Feb. 1988.
- ⁷Bray, D., and Knowles, K., "Normal Impinging Jet in Crossflow—a Parametric Investigation," AIAA/ASME/SAE/ASEE 25th Joint Propulsion Conf., AIAA Paper 89-2957, Monterey, CA, July 1989.
- ⁸Green, L., private communication, British Aerospace (Military Aircraft) Ltd., Warton, England, UK, Nov. 1988.
- ⁹Stott, M. R., private communication, British Aerospace (Military Aircraft) Ltd., Warton, England, UK, Nov. 1988.
- ¹⁰MacLean, R., Sullivan, J., and Murthy, S. N. B., "Hot Gas Environment Around STOVL Aircraft in Ground Proximity—Part I: Experimental Study," AIAA/ASME/SAE/ASEE 26th Joint Propulsion Conf., AIAA Paper 90-2269, Orlando, FL, July 16–18, 1990.
- ¹¹Smith, A. G., Ing, D. N., and Bailey, P. J., "The Experimental and Computational Study of Jet Impingement Flowfields with Reference to VSTOL Aircraft Performance," Royal Aeronautical Society International Powered Lift Conf., London, Aug. 29–31, 1990.
- ¹²Barata, J. M. M., Durao, D. F. G., and McGuirk, J. J., "Numerical Study of Single Impinging Jets Through a Crossflow," *Journal of Aircraft*, Vol. 26, No. 11, 1989, pp. 1002–1008.
- ¹³Tafti, D., and Vanka, S. P., "Hot Gas Environment Around STOVL Aircraft in Ground Proximity—Part II: Numerical Study," AIAA/ASME/SAE/ASEE 26th Joint Propulsion Conf., AIAA Paper 90-2270, Orlando, FL, July 16–18, 1990.
- ¹⁴Van Dalsem, W. R., Chawla, K., and Smith, M. H., "Numerical Simulation of Powered-Lift Flows," Royal Aeronautical Society International Powered Lift Conf., London, Aug. 29–31, 1990.
- ¹⁵Knowles, K., Bray, D., Bailey, P. J., and Curtis, P., "Impinging Jets in Crossflow," Royal Aeronautical Society International Powered Lift Conf., London, Aug. 29–31, 1990; see also, *The Aeronautical Journal*, Vol. 96, No. 952, 1992, pp. 47–56.
- ¹⁶Tidball, I. C., "V/STOL Aerodynamics," Royal Military College of Science, 42 Degree Course Aeromechanical Systems Engineering Project Rept., Wiltshire, England, UK, May 1990.
- ¹⁷Abbott, W. A., and White, D. R., "The Effect of Nozzle Pressure Ratio on the Fountain Formed Between Two Impinging Jets," Royal Aerospace Establishment TM P 1166, Pyestock, England, UK, May 1989.
- ¹⁸Barata, J. M. M., private communication, Instituto Superior Técnico, Lisbon, Portugal, 1990.
- ¹⁹Bray, D., and Knowles, K., "Experimental Investigations into Twin Impinging Jets in Cross-Flows," 18th Congress of the International Council of the Aeronautical Sciences, ICAS-92-4.8.3, Beijing, People's Republic of China, Sept. 20–25, 1992.
- ²⁰Donaldson, C. du P., and Snedeker, R. S., "A Study of Free Jet Impingement, Part 1, Mean Properties of Free and Impinging Jets," *Journal of Fluid Mechanics*, Vol. 45, No. 2, 1971, pp. 281–319.